Frontiers of Information Technology & Electronic Engineering
www.zju.edu.cn/jzus; engineering.cae.cn; www.springerlink.com
ISSN 2095-9184 (print); ISSN 2095-9230 (online)
E-mail: jzus@zju.edu.cn

Application of direct adaptive fuzzy sliding mode control into a class of non-affine discrete nonlinear systems*#

Xiao-yu ZHANG
(*School of Electronic and Information Engineering, North China Institute of Science and Technology, Beijing 101601, China*)
E-mail: xyzhang@iipc.zju.edu.cn

Received Oct. 3, 2015; Revision accepted Apr. 7, 2016; Crosschecked Dec. 2, 2016

Abstract: Direct adaptive fuzzy sliding mode control design for discrete non-affine nonlinear systems is presented for trajectory tracking problems with disturbance. To obtain adaptiveness and eliminate chattering of sliding mode control, a dynamic fuzzy logical system is used to implement an equivalent control, in which the parameters are self-tuned online. Stability of the sliding mode control is validated using the Lyapunov analysis theory. The overall system is adaptive, asymptotically stable, and chattering-free. A numerical simulation and an application to a robotic arm with two degrees of freedom further verify the good performance of the control design.

Key words: Nonlinear system, Discrete system, Dynamic fuzzy logical system, Direct adaptive, Sliding mode control
http://dx.doi.org/10.1631/FITEE.1500318 **CLC number:** TP273

1 Introduction

Sliding mode control (SMC) is an important control method because of its robustness, invariance to uncertainties, and resistance to external disturbance (Utkin, 1977; Sira-Ramirez, 1989; Edwards and Spurgeon, 1998). Over the past several decades, SMC has attracted major research interest and has been widely applied to many industrial processes, such as flying craft control, motor drive, and chemical engineering. In recent years, many researchers have begun to investigate the application of SMC into adaptive control and intelligent control methods, such as the combination of SMC with neural networks (Morioka *et al.*, 1995) or with fuzzy logic systems (Zhang and Panda, 1999). Particularly, in the field of fuzzy logic control, its combination with SMC can be used to overcome an obvious shortcoming, namely, the chattering phenomenon that impedes the application of SMC.

Fuzzy logic control (FLC) has been specifically widely applied to the practical control systems, in which the precise mathematic model cannot be acquired easily. Fuzzy logic systems (FLSs) are applied to sliding mode control systems in order to improve the performance of SMC, and to approximate unknown dynamic functions or eliminate chattering in particular. Since FLS has a great approximation ability, it has wide potential applications in many control design fields with fast development. Numerous studies have been done related to online or offline identification for nonlinear dynamics (Wang, 1995; Lee and Vukovich, 1997; Wang and Yu, 2000). To improve the performance of SMC, FLS is applied

* Project supported by the National Natural Science Foundation of China (No. 61304024), the Science and Technology Project of Hebei Province, China (No. 15272118), and the Fundamental Research Funds for the Central Universities, China (No. 3142015101)
# A preliminary version was presented at the 12th International Conference on Fuzzy Systems and Knowledge Discovery, Zhangjiajie, China, Aug. 15–17, 2015
ORCID: Xiao-yu ZHANG, http://orcid.org/0000-0003-1436-8116

into SMC design. Such a combination approach is also known as fuzzy sliding mode control (FSMC).

FSMC has very wide applications. For example, the chaos SMC of a class of fractional-order chaotic systems was propounded (Chen *et al.*, 2012a). Then a new FSMC method was proposed for different initial conditions and different dimensions (Chen *et al.*, 2012b). Hwang *et al.* (2009) applied the FSMC to an electric bicycle system. They employed two scaling factors to normalize the sliding surface and its derivative, and adopted an appropriate 'if-then' rule for the FLS. Such a method can help deal with huge uncertainties of the bicycle system. In the situation of unavailable state information, Wang and Liu (2010) proposed an FSMC design based on a sliding mode estimator. Zhu and Li (2010) proposed a decentralized FSMC for manipulators. Many other FSMC related applications were proposed, such as the development of hydraulic pressure coupling drive systems (Ho and Ahn, 2012), uncertain micro-electromechanical systems (Yau *et al.*, 2011), and nonlinear chemical processes (Shahraz and Boozarjomehry, 2009).

On the other hand, the use of the SMC principle to construct fuzzy 'if-then' rules might lead to sliding mode fuzzy logic control (SMFC). For example, for the control of a digital signal processor based (DSP-based) boost converter, Guo *et al.* (2011) proposed an SMFC design which encompasses the desirable characteristics of both fuzzy and sliding mode controllers. Experimental results were assessed compared to the cases when a linear PID or PI controller was used. Poursamad and Davaie-Markazi (2009) proposed a robust adaptive fuzzy control algorithm, which consists of an FLS and a robust controller, and applied it to unknown chaotic systems. Particularly, the fuzzy logic system was designed based on the sliding mode control with all parameters adaptively tuned. Hsu *et al.* (2009) proposed a self-regulating fuzzy control (SRFC) design method using a gradient rule modification method to regulate the fuzzy rules. Also, a self-regulating fuzzy sliding mode control (SRFSMC) design method was developed (Hsu *et al.*, 2009) that could be used to control a forward DC-DC converter. Zhang (2009) proposed an extending sliding mode-like fuzzy logic control (SMLFC) method for nonlinear systems. Allaoua and Laoufi (2013) proposed a new FLC based on sliding mode by taking the advantage of support vector machines (SVMs), and applied it to an electric vehicle propulsion system. Farhoud and Erfanian (2014) proposed an FLC method based on a higher-order sliding mode, which demonstrated excellent transient and steady-state responses.

These FSMC or SMFC designs are clearly successful in practical use. The advantages of the SMC and the FLC controllers could be integrated, and their disadvantages could be reduced or even removed. However, most of the above-mentioned studies just considered continuous systems, whereas FSMC or SMFC designs for discrete nonlinear systems were sporadically reported. In practice, the control scheme is always implemented by a computer or a DSP apparatus. Therefore, the discrete sliding mode control (DSMC) has high potential in engineering, and it could be conveniently applied for the realization of digital devices, so that a sampled data system could be established. Numerous studies have been carried out in the field of DSMC over a long period (Sarpturk *et al.*, 1987; Furuta, 1990; Monsees and Scherpen, 2002; Reddy *et al.*, 2009; Corradini *et al.*, 2012; Khandekar *et al.*, 2013; Pande *et al.*, 2013; Lian *et al.*, 2014; Pai, 2014; Zhang and Guo, 2014).

SMC has one obvious drawback, i.e., the chattering phenomenon, which would significantly impede its practical application. In particular, the chattering becomes more serious for discrete systems due to the processes of sampling, digitization of analog signals, and complicated discrete modeling (Castillo-Toledo *et al.*, 2008). Monsees and Scherpen (2002) put forward a method of online tuning the switching gain by an adaptive law, so that the chattering for the concerned discrete systems could be reduced. Another problem in engineering practice is the unknown precise model dynamics. Fortunately, FLS has a great approximation ability and it has a filtering function to deal with such problems. Therefore, the combination of SMC and FLS is a proper approach to dealing with discrete nonlinear systems, especially for those systems with unknown dynamics. As for online control applications, however, a key point is to seek a proper adaptive law.

In this study, we consider a class of non-affine discrete nonlinear systems with an adaptive FSMC design specifically presented. For a discrete nonlinear system with unknown nonlinear dynamic functions, a dynamic fuzzy logic system (DFLS), for which the parameters are self-tuned by the adaptive laws, is first constructed to approximate the unknown dynamics. The SMC controller is designed based on the DFLS. The stability of the tracking error and the reaching condition of the sliding mode are then validated using the Lyapunov stability theory.

This paper is an extension of Zhang *et al.* (2015). The contributions of the current work are listed as follows:

1. The analysis and discussion of the disturbance are elaborated to further clarify the significance of the discrete model considered in this paper. The assumption of the disturbance is revised, which further relaxes the model condition and makes the method adapt to more general applications.

2. The adaptive DFLS design is extended in detail and the parameters of the forward and backward parts are clearly designed.

3. The main results achieve more strict and rigorous improvements. First, in the DFLS design for approximation, relations of the estimated function, its optimal approximation, and the absolute error are clearly clarified. The point is very important for the rigorous controller design (Theorem 1). Second, the parameter design of the controller and the adaptive law are improved. Under the same tuning condition ($\alpha_i > 0$, $0 < \beta_i < 1$), the controller parameters ($k_{i,1}$, $k_{i,2}$) have been simplified. Again, the chattering problem is considered with analysis and discussion. Chattering depends on the absolute approximation error. Fortunately, this value is very small due to the strong approximation ability of the DFLS. Therefore, the proposed design method has nearly no chattering.

4. An application to a robotic arm with two degrees of freedom is added via simulation.

2 Problem formulation

Consider a class of discrete nonlinear systems:

$$\boldsymbol{y}_k^{(r)} = f(\boldsymbol{x}_k, \boldsymbol{u}_k) + d(\boldsymbol{x}_k), \tag{1}$$

where $\boldsymbol{y}_k = [y_{1,k}, y_{2,k}, \dots, y_{m,k}]^{\mathrm{T}}$ denotes the output vector, $\boldsymbol{r} = [r_1, r_2, \dots, r_m]^{\mathrm{T}}$ with each element r_i denoting a subsystem's relative degree (the total relative degree $n = \sum_{i=1}^m r_i$), and $\boldsymbol{u}_k = [u_{1,k}, u_{2,k}, \dots, u_{m,k}]^{\mathrm{T}}$ denotes the control input vector. The system state vector is $\boldsymbol{x}_k = [\boldsymbol{y}_{1,k}^{\mathrm{T}}, \boldsymbol{y}_{2,k}^{\mathrm{T}}, \dots, \boldsymbol{y}_{m,k}^{\mathrm{T}}]^{\mathrm{T}}$ with $\boldsymbol{y}_{i,k} = [y_{i,k}, y_{i,k+1}, \dots, y_{i,k+r_i-1}]^{\mathrm{T}}$ for $i = 1, 2, \dots, m$. Consequently, $\boldsymbol{y}_k^{(r)} = [y_{1,k}^{(r_1)}, y_{2,k}^{(r_2)}, \dots, y_{m,k}^{(r_m)}]^{\mathrm{T}}$ denotes its forward difference vector with $y_{i,k}^{(r_i)} = y_{i,k+r_i}$ ($i = 1, 2, \dots, m$). Additionally,

$$\begin{aligned} f(\boldsymbol{x}_k, \boldsymbol{u}_k) =& [f_1(\boldsymbol{x}_k, u_{1,k}), f_2(\boldsymbol{x}_k, u_{2,k}), \\ & \dots, f_m(\boldsymbol{x}_k, u_{m,k})]^{\mathrm{T}} \end{aligned}$$

is defined as the nonlinear dynamic vector, whose components $f_i(\boldsymbol{x}_k, u_{i,k}) \in L^2(\mathbb{R})$ ($i = 1, 2, \dots, m$) are unknown. Moreover,

$$d(\boldsymbol{x}_k) = [d_1(\boldsymbol{x}_k), d_2(\boldsymbol{x}_k), \dots, d_m(\boldsymbol{x}_k)]^{\mathrm{T}}$$

represents the unknown disturbance or unmodeled dynamics.

The disturbance $d(\boldsymbol{x}_k)$ in the controlled system (1), which has relation with only the system state $\boldsymbol{x}_k$, is certainly unknown and is not required to be bounded. It is only a type of interference to the state equation, related with the state $\boldsymbol{x}_k$ itself and affecting the movement of the system state $\boldsymbol{x}_k$. Therefore, if the adaptive mechanism has the ability of tracking it, this kind of effect can be treated. In this study, the disturbance $d(\boldsymbol{x}_k)$ is considered as part of the unknown dynamics, which can be approximated by the DFLS online. Then the SMC controller is not required to consider that the disturbance is matched or unmatched, or compensated by the switching signal (the nonlinear part of the SMC).

The subscript i represents every branch of the subsystem and the subscript k denotes the discrete time instant. If $\bar{\boldsymbol{y}}_k = [\bar{y}_{1,k}, \bar{y}_{2,k}, \dots, \bar{y}_{m,k}]^{\mathrm{T}}$ represents the trajectory to be tracked and comprises the following vectors:

$$\bar{\boldsymbol{y}}_{i,k} = [\bar{y}_{i,k}, \bar{y}_{i,k+1}, \dots, \bar{y}_{i,k+r_i-1}]^{\mathrm{T}},\ i = 1, 2, \dots, m,$$

the tracked mathematic model is described by

$$\bar{y}_{i,k}^{(r_i)} = -\sum_{j=0}^{r_i-1} a_j \bar{y}_{i,k+j} + r_i(k), \tag{2}$$

where $\bar{y}_{i,k}^{(r_i)} = \bar{y}_{i,k+r_i}$ ($i = 1, 2, \dots, m$) with a_j ($j = 0, 1, \dots, r_i - 1$) being Hurwitz coefficients and $r_i(k)$ the reference signal. The control problem is to design a controller for system (1) such that the tracking error is

$$\boldsymbol{e}_k = [\boldsymbol{e}_{1,k}^{\mathrm{T}}, \boldsymbol{e}_{2,k}^{\mathrm{T}}, \dots, \boldsymbol{e}_{m,k}^{\mathrm{T}}]^{\mathrm{T}}, \tag{3}$$

where each element

$$\boldsymbol{e}_{i,k} = \boldsymbol{y}_{i,k} - \bar{\boldsymbol{y}}_{i,k} = [e_{i,k}, e_{i,k+1}, \dots, e_{i,k+r_i-1}]^{\mathrm{T}} \tag{4}$$

with $e_{i,k} = y_{i,k} - \bar{y}_{i,k}$ $(i = 1, 2, \ldots, m)$ converges to the origin asymptotically.

By the above definitions, we obtain $e_{i,k+r_i}$ from Eqs. (1)–(4) as

$$e_{i,k+r_i} = f_i(\boldsymbol{x}_k, u_{i,k}) + d_i(\boldsymbol{x}_k) + \sum_{j=0}^{r_i-1} a_j \bar{y}_{i,k+j} - r_i(k). \tag{5}$$

The sliding manifolds are defined as follows:

$$\boldsymbol{S}_k = [S_{1,k}, S_{2,k}, \ldots, S_{m,k}]^{\mathrm{T}}, \tag{6}$$

where

$$S_{i,k} = \boldsymbol{C}_i \boldsymbol{e}_{i,k},\ i = 1, 2, \ldots, m, \tag{7}$$

with $\boldsymbol{C}_i = [c_{i,1}, c_{i,2}, \ldots, c_{i,r_i}]^{\mathrm{T}}$ satisfying the discrete Hurwitz polynomial:

$$h_i(\cdot) = c_{i,r_i} e_{i,k+r_i-1} + c_{i,r_i-1} e_{i,k+r_i-2} + \ldots + c_{i,1} e_{i,k}.$$

We aim to look for a design of the fuzzy adaptive sliding mode controller:

$$u_{i,k} = u_{\mathrm{eq},i} + u_{v,i},\ i = 1, 2, \ldots, m, \tag{8}$$

where $u_{\mathrm{eq},i}$ is the equivalent control and $u_{v,i}$ the hitting control such that the manifold $S_{i,k}$ can be reached. Because function $f_i(\boldsymbol{x}_k, u_{i,k})$ is unknown, the control input $u_{i,k}$ cannot be designed directly. In the following section, a DFLS will be adopted to realize an SMC controller.

The following assumptions are necessary to underlie the remainder of this study:

Assumption 1 The function $f_i(\boldsymbol{x}_k, u_{i,k}) \in L^2(\mathbb{R})$ and

$$f_{i,u_i} \stackrel{\mathrm{def}}{=} \frac{\partial f_i(\boldsymbol{x}_k, u_{i,k})}{\partial u_{i,k}} \neq 0,\ \forall\ \boldsymbol{x}_k \in \Omega_{\boldsymbol{x}_k},$$

where $\Omega_{\boldsymbol{x}_k}$ is the compact set of state $\boldsymbol{x}_k$.

For all $\boldsymbol{x}_k \in \Omega_{\boldsymbol{x}_k}$, the smooth function satisfies $f_{i,u_i} > 0$ or $f_{i,u_i} < 0$. Without loss of generality, it is assumed $f_{i,u_i} > 0$.

Assumption 2 There exists a positive upper bound function $\bar{b}_i(\boldsymbol{x}_k)$ such that $\forall \boldsymbol{x}_k \in \Omega_{\boldsymbol{x}_k}$, $0 < f_{i,u_i} \leq \bar{b}_i(\boldsymbol{x}_k)$.

Assumption 3 The unknown disturbance or unmodeled dynamic $d_i(\boldsymbol{x}_k) \in L^2(\mathbb{R}),\ i = 1, 2, \ldots, m$.

The constraint condition for $d_i(\boldsymbol{x}_k)$ is released compared with that mentioned in Zhang *et al.* (2015). In general, $d_i(\boldsymbol{x}_k)$ is required to be bounded, and we should confirm that the function to be estimated is bounded. Only in this way, can Lemma 1 (given later) be used. Hence, there is Assumption 3 in Zhang *et al.* (2015). However, in this study the function to be estimated is $g_{i,k}(\boldsymbol{x}) \in L^2(\mathbb{R})$, if we suppose $d_i(\boldsymbol{x}_k) \in L^2(\mathbb{R})$ (Eq. (11)). So, the function $g_{i,k}(\boldsymbol{x})$ can be approximated optimally by the DFLS. Therefore, the constraint condition becomes Assumption 3 in the current paper, which releases the condition for the unknown disturbance or unmodeled dynamics.

3 Dynamic fuzzy logic system design

Using the singleton fuzzifier, product inference rule, and average defuzzifier method, a dynamic fuzzy logic system (DFLS) can be described as follows (Lee and Vukovich, 1997). However, since system (1) is discrete, we adopt a discrete DFLS as follows:

$$\hat{g}(\boldsymbol{x}, \tau+1) = -\xi[\hat{g}(\boldsymbol{x}, \tau) - \boldsymbol{\Theta}^{\mathrm{T}}(\tau)\, \boldsymbol{p}(\boldsymbol{x})], \tag{9}$$

where $\hat{g}(\boldsymbol{x})$ is the approximation of $g(\boldsymbol{x})$ (a nonlinear scalar function to be approximated), τ is the sampling time interval of the DFLS which is different from the sampling time interval k of system (1), $\boldsymbol{\Theta}(\tau) = [\theta_1(\tau), \theta_2(\tau), \ldots, \theta_M(\tau)]^{\mathrm{T}}$ is the support point vector of the fuzzy rule base, being an adjustable parameter of the fuzzifier of the DFLS, $\xi > 0$ is a real scalar parameter to be designed, and $\boldsymbol{p}(\boldsymbol{x}) = [p_1(\boldsymbol{x}), p_2(\boldsymbol{x}), \ldots, p_M(\boldsymbol{x})]^{\mathrm{T}}$ is the fuzzy basis function vector. The element of the fuzzy basis function is determined by

$$p_l(\boldsymbol{x}) = \frac{\prod_{j=1}^{N} \mu_j^l}{\sum_{l=1}^{M} \prod_{j=1}^{N} \mu_j^l}, \tag{10}$$

where M is the number of fuzzy rules and N the number of input variables of the DFLS. The input variables of the DFLS are selected as state variables of the system with $\boldsymbol{x}_k = [x_{1,k}, x_{2,k}, \ldots, x_{n,k}]^{\mathrm{T}}$. Obviously, in this case $N = n$.

The membership functions of input variables are all triangular (Fig. 1). In the figure, φ_j $(j = 1, 2, \ldots, n)$, which are set up by the designer, are the fuzzy partition parameters of the input variables. The universe field partitions and the triangular membership function of the output variables

$\hat{g}(\boldsymbol{x})$ are shown in Fig. 2. We adopt the product inferring method, resulting in the following fuzzy inference rules:

If $x_{1,k}$ is a_1^1, $x_{2,k}$ is a_2^1, ..., and $x_{n,k}$ is a_N^1, then $\hat{g}(\boldsymbol{x})$ is θ_1;

If $x_{1,k}$ is a_1^2, $x_{2,k}$ is a_2^2, ..., and $x_{n,k}$ is a_N^2, then $\hat{g}(\boldsymbol{x})$ is θ_2;

...

If $x_{1,k}$ is a_1^M, $x_{2,k}$ is a_2^M, ..., and $x_{n,k}$ is a_N^M, then $\hat{g}(\boldsymbol{x})$ is θ_M.

A weighted averaging defuzzifier is adopted. Therefore, the fuzzy rule base (10) is obtained, where p_l is the lth rule membership value of the output variable $\hat{g}(\boldsymbol{x})$. Here, $l = 1, 2, \ldots, 3^n$ is the number of rules, i.e., $M = 3^n$. According to the fuzzy rules and the output variable partitions (Fig. 2), the support point vector element of the fuzzy rule base is obtained as $\forall i = 1, 2, \ldots, M$, $\theta_i = \phi_q$ for $q = 1, 2, \ldots, 5$. Therefore, the support point vector of the fuzzy rule base, $\boldsymbol{\Theta}(\tau) = [\theta_1(\tau), \theta_2(\tau), \ldots, \theta_M(\tau)]^{\mathrm{T}}$, is essentially the partition parameter of the defuzzifier, which will be self-tuned online by the adaptive law for approximation.

The following Lemma is introduced for its application in this study (Wang, 1995):

Lemma 1 For smooth nonlinear vector field $g(\boldsymbol{x})$: $\mathbb{R}^n \to \mathbb{R}$, there is a parameter

$$\boldsymbol{\Theta}^* = \arg\min_{\theta\in\Omega_\theta}\left[\sup_{\boldsymbol{x}\in\mathbb{R}^n}\|g(\boldsymbol{x}) - g^*(\boldsymbol{x})\|\right]$$

to guarantee $\forall\varepsilon \in \mathbb{R}$, $\varepsilon > 0$, $\|g(\boldsymbol{x}) - g^*(\boldsymbol{x})\| < \varepsilon$, where $g^*(\boldsymbol{x})$ is the approximation output of DFLS (9), namely $g^*(\boldsymbol{x}) = (\boldsymbol{\Theta}^*)^{\mathrm{T}}\boldsymbol{p}$.

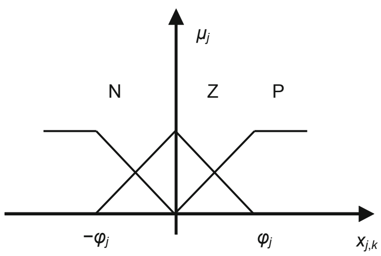

Fig. 1 Fuzzy sets of the input variables in the dynamic fuzzy logic system (N: negative; Z: zero; P: positive)

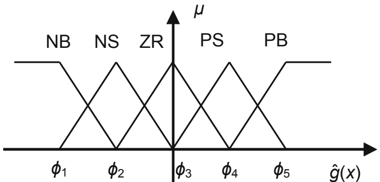

Fig. 2 Fuzzy sets of the output variables in the dynamic fuzzy logic system (NB: negative big; NS: negative small; ZR: zero; PS: positive small; PB: positive big)

In the SMC controller design, the DFLS described by Eq. (9) and the above rules of the fuzzy logic system are adopted for the approximation of unknown dynamics.

4 Main results

We use the DFLS described by Eq. (9) to approximate the unknown dynamics, so that the equivalent control can be obtained. Then the approximation error can be compensated by the hitting control design.

4.1 Adaptive sliding mode control law design

The objective is to design a sliding mode controller $u_{i,k}$ (Eq. (8)) such that $S_{i,k} = 0$. The SMC controller requires a method to approximate those unknown dynamics. Here, the approach of function approximation described in Section 3 which is based on the DFLS will be adopted to approximate the unknown dynamics. In the following analysis, only one branch $S_{i,k}$ of the sliding mode $\boldsymbol{S}_k$ and one control input branch $u_{i,k}$ will be processed for convenience. To carry out the subsequent control law design, the following Lemma is introduced (Zhang and Su, 2004):

Lemma 2 For Hurwitz polynomial parameters $c_{i,j} > 0$ $(j = 1, 2, \ldots, r_i - 1)$ and $c_{i,r_i} > 0$, there are always parameters $\lambda_{i,j} > 0$ $(j = 0, 1, \ldots, r_i)$ which guarantee

$$\boldsymbol{D}_i = \begin{bmatrix} \lambda_{i,0} & 0 & \cdots & 0 & c_{i,1} \\ 0 & \lambda_{i,1} & \cdots & 0 & c_{i,2} \\ \vdots & \vdots & & \vdots & \vdots \\ 0 & 0 & \cdots & \lambda_{i,r_i-1} & c_{i,r_i} \\ c_{i,1} & c_{i,2} & \cdots & c_{i,r_i} & \lambda_{i,r_i} \end{bmatrix} > 0$$

and $\boldsymbol{D}_i = \boldsymbol{D}_i^{\mathrm{T}}$.

For the convenience of the design, we define

$$\begin{aligned} S_{i,a}(k) =& \frac{1}{2}\sum_{j=0}^{r_i-1}\lambda_{i,j}\left(e_{i,k+j}^2 - e_{i,k+j-1}^2\right) \\ & - \frac{\lambda_{i,r_i}}{2}e_{i,k+r_i-1}^2 - S_{i,k-1}e_{i,k+r_i-1}, \end{aligned}$$

and define a nonlinear dynamic function

$$g_{i,k}(\boldsymbol{x}) = \left(S_{i,k}\bar{b}_i\left(\boldsymbol{x}_k\right)\right)^{-1}\left(S_{i,a}\left(k\right) + 0.5\lambda_{i,r_i}e_{i,k+r_i}^2\right) + \left(\bar{b}_i(\boldsymbol{x}_k)\right)^{-1}\left(f_i(\boldsymbol{x}_k, u_{i,k}) + d_i(\boldsymbol{x}_k)\right) - u_{i,k}, \tag{11}$$

which will be approximated as $\hat{g}_{i,k}(\boldsymbol{x})$ by the DFLS.

According to Lemma 1, there is a parameter $\boldsymbol{\Theta}_i^*$ such that

$$\forall\varepsilon \in \mathbb{R},\ \varepsilon > 0,\ \left\|g_{i,k}(\boldsymbol{x}) - \hat{g}_{i,k}^*(\boldsymbol{x})\right\| < \varepsilon, \tag{12}$$

where $\hat{g}_{i,k}^*(\boldsymbol{x})$ is the approximation output of the fuzzy logic system, namely,

$$\hat{g}_{i,k}^*(\boldsymbol{x}) = (\boldsymbol{\Theta}^*)^{\mathrm{T}}\boldsymbol{p}. \tag{13}$$

Therefore, we have the following relationship:

$$g_{i,k}(\boldsymbol{x}) = \hat{g}_{i,k}^*(\boldsymbol{x}) \pm \varepsilon, \tag{14}$$

where ε is the absolute value of the minimum approximation error.

Consequently, an SMC controller is designed as

$$u_{i,k} = -\left(\bar{b}_i(\boldsymbol{x}_k)\right)^{-1}\sum_{j=0}^{r_i-1} a_j\bar{y}_{i,k+j} + \left(\bar{b}_i(\boldsymbol{x}_k)\right)^{-1} r_i(k) - \hat{g}_{i,k}(\boldsymbol{x}) - \left\{\varepsilon_{i,h} + \left[k_{i,1} + k_{i,2}\bar{b}_i(\boldsymbol{x}_k)\right]|S_{i,k}|\right\}\mathrm{sgn}(S_{i,k}), \tag{15}$$

where $\mathrm{sgn}(\cdot)$ is the sign function with parameters

$$\varepsilon_{i,h} > |\varepsilon|,\ \ k_{i,1} > 0,\ \ k_{i,2} > \frac{\alpha_i}{2\beta_i} + \frac{\beta_i}{2}\|\boldsymbol{G}_i\|^{-1}. \tag{16}$$

Here, $\boldsymbol{G}_i \in \mathbb{R}^{M\times M}$ is an optional parameter matrix satisfying $\boldsymbol{G}_i = \boldsymbol{G}_i^{\mathrm{T}}$ and $\boldsymbol{G}_i > 0$, and $\alpha_i > 0$, $0 < \beta_i < 1$ are optional scalar parameters.

To approximate the unknown nonlinear dynamic function $g_{i,k}(\boldsymbol{x})$ online, the adaptive laws of the adopted DFLS are designed as follows:

$$\begin{cases} \Delta\boldsymbol{\Theta}_i\left(k\right) = \beta_i\boldsymbol{G}_i^{-\mathrm{T}}\boldsymbol{p}S_{i,k}\bar{b}_i(\boldsymbol{x}_k), \\ \Delta\hat{g}_{i,k}(\boldsymbol{x}) = -\left(1-\beta_i\right)\left[\hat{g}_{i,k}(\boldsymbol{x}) - \left(\boldsymbol{\Theta}_i(k)\right)^{\mathrm{T}}\boldsymbol{p}\right] \\ \qquad + \left(\alpha_i + \beta_i\boldsymbol{p}^{\mathrm{T}}\boldsymbol{G}_i^{-\mathrm{T}}\boldsymbol{p}\right)S_{i,k}\bar{b}_i(\boldsymbol{x}_k). \end{cases} \tag{17}$$

Following the above definitions and Eq. (11), we can obtain the following equation:

$$S_{i,k}\bar{b}_i(\boldsymbol{x}_k)g_{i,k}(\boldsymbol{x}) = S_{i,a}\left(k\right) + 0.5\lambda_{i,r_i}e_{i,k+r_i}^2 + S_{i,k}\left[f_i(\boldsymbol{x}_k, u_{i,k}) + d_i(\boldsymbol{x}_k)\right] - S_{i,k}\bar{b}_i(\boldsymbol{x}_k)u_{i,k}.$$

Substituting the designed controller (15) into the above and using Eq. (5), we have

$$S_{i,k}\bar{b}_i(\boldsymbol{x}_k)\left(g_{i,k}(\boldsymbol{x}) - \hat{g}_{i,k}(\boldsymbol{x})\right) = S_{i,a}\left(k\right) + 0.5\lambda_{i,r_i}e_{i,k+r_i}^2 + S_{i,k}e_{i,k+r_i} + \varepsilon_{i,h}\left|S_{i,k}\right|\bar{b}_i(\boldsymbol{x}_k) + \left[k_{i,1}\bar{b}_i(\boldsymbol{x}_k) + k_{i,2}\left(\bar{b}_i(\boldsymbol{x}_k)\right)^2\right]\left|S_{i,k}\right|^2. \tag{18}$$

It will be used for stability analysis in the following subsection.

According to Lemma 1, the approximation error will be arbitrarily small. Then $\varepsilon_{i,h}$ can be selected as any real size according to the situation of system uncertainties and disturbance. In Eq. (17), the first formula describes the adaptive mechanism, and the second one describes the DFLS. From these two formulas, it can be seen that both the operation of the DFLS and the adaptive mechanism need the sliding mode value $S_{i,k}$. When the system state reaches the sliding mode, i.e., $S_{i,k} = 0$, the adaptive mechanism is in a steady state. The SMC controllers (11)–(16) constitute a complex dynamic subsystem. In the following, the analysis of the closed-loop system stability is carried out.

4.2 Stability analysis

The main result of system stability is summarized in the following theorem:

Theorem 1 Given nonlinear system (1) and reference trajectory (2), the sliding modes (6) and (7) are reachable and the system tracking errors (3) and (4) are globally asymptotically stable under the FSMC controllers (11)–(16), which are based on the DFLS (Eqs. (9), (10), and (17)), if the coefficients of sliding modes (6) and (7), $c_{i,j} > 0$ ($i = 1, 2, \ldots, m,\ j = 1, 2, \ldots, r_i$), are Hurwitz.

Proof Choose the Lyapunov function of the tracking error as

$$V_{i,k} = \frac{\alpha_i\beta_i}{2}\tilde{\boldsymbol{e}}_{i,k}^{\mathrm{T}}\boldsymbol{D}_i\tilde{\boldsymbol{e}}_{i,k} + \frac{1}{2}\left[\hat{g}_{i,k}(\boldsymbol{x}) - (\boldsymbol{\Theta}_i(k))^{\mathrm{T}}\boldsymbol{p}\right]^2 + \frac{\alpha_i}{2}\tilde{\boldsymbol{\Theta}}_i^{\mathrm{T}}\boldsymbol{G}_i\tilde{\boldsymbol{\Theta}}_i, \tag{19}$$

where

$$\tilde{\boldsymbol{e}}_{i,k} = \left[e_{i,k-1}, e_{i,k}, \ldots, e_{i,k+r_i-1}\right]^{\mathrm{T}}$$

and $\tilde{\boldsymbol{\Theta}}_i = \boldsymbol{\Theta}_i^* - \boldsymbol{\Theta}_i(k)$ is the error between $\boldsymbol{\Theta}_i(k)$ and the optimum parameter $\boldsymbol{\Theta}_i^*$. According to Lemma 2, we have $\boldsymbol{D}_i = \boldsymbol{D}_i^{\mathrm{T}}$, $\boldsymbol{D}_i > 0$, and $V_{i,k} > 0$. Furthermore, when $\|\tilde{\boldsymbol{e}}_{i,k}\| \to \infty$, $|V_{i,k}| \to \infty$.

Seeking the time difference of the Lyapunov function (19), we have

$$\Delta V_{i,k} = \alpha_i\beta_i\left[S_{i,a}(k) + S_{i,k}e_{i,k+r_i} + \frac{\lambda_{i,r_i}}{2}e_{i,k+r_i}^2\right]$$
$$+ \frac{\alpha_i}{2}[\boldsymbol{\Theta}_i^* - \boldsymbol{\Theta}_i(k+1)]^{\mathrm{T}}\boldsymbol{G}_i[\boldsymbol{\Theta}_i^* - \boldsymbol{\Theta}_i(k+1)]$$
$$- \frac{\alpha_i}{2}[\boldsymbol{\Theta}_i^* - \boldsymbol{\Theta}_i(k)]^{\mathrm{T}}\boldsymbol{G}_i[\boldsymbol{\Theta}_i^* - \boldsymbol{\Theta}_i(k)]$$
$$+ \frac{1}{2}\left[\hat{g}_{i,k+1}(\boldsymbol{x}) - (\boldsymbol{\Theta}_i(k+1))^{\mathrm{T}}\boldsymbol{p}\right]^2$$
$$- \frac{1}{2}\left[\hat{g}_{i,k}(\boldsymbol{x}) - (\boldsymbol{\Theta}_i(k))^{\mathrm{T}}\boldsymbol{p}\right]^2.$$

Then substituting the adaptive law (17) into the above equation, we have

$$\Delta V_{i,k} = \alpha_i\beta_i\left[S_{i,a}(k) + S_{i,k}e_{i,k+r_i} + \frac{\lambda_{i,r_i}}{2}e_{i,k+r_i}^2\right]$$
$$+ \frac{\alpha_i}{2}\left[\boldsymbol{\Theta}_i^* - \boldsymbol{\Theta}_i(k) - \beta_i\boldsymbol{G}_i^{-\mathrm{T}}\boldsymbol{p}S_{i,k}\bar{b}_i(\boldsymbol{x}_k)\right]^{\mathrm{T}}\boldsymbol{G}_i$$
$$\cdot\left[\boldsymbol{\Theta}_i^* - \boldsymbol{\Theta}_i(k) - \beta_i\boldsymbol{G}_i^{-\mathrm{T}}\boldsymbol{p}S_{i,k}\bar{b}_i(\boldsymbol{x}_k)\right]$$
$$- \frac{\alpha_i}{2}[\boldsymbol{\Theta}_i^* - \boldsymbol{\Theta}_i(k)]^{\mathrm{T}}\boldsymbol{G}_i[\boldsymbol{\Theta}_i^* - \boldsymbol{\Theta}_i(k)]$$
$$+ \frac{1}{2}\Big\{\hat{g}_{i,k}(\boldsymbol{x}) - (1-\beta_i)\left[\hat{g}_{i,k}(\boldsymbol{x}) - (\boldsymbol{\Theta}_i(k))^{\mathrm{T}}\boldsymbol{p}\right]$$
$$+\alpha_i S_{i,k}\bar{b}_i(\boldsymbol{x}_k) - (\boldsymbol{\Theta}_i(k))^{\mathrm{T}}\boldsymbol{p}\Big\}^2$$
$$- \frac{1}{2}\left[\hat{g}_{i,k}(\boldsymbol{x}) - (\boldsymbol{\Theta}_i(k))^{\mathrm{T}}\boldsymbol{p}\right]^2.$$

Continuing simplifying the above, we have

$$\Delta V_{i,k} = \alpha_i\beta_i\left[S_{i,a}(k) + S_{i,k}e_{i,k+r_i} + \frac{\lambda_{i,r_i}}{2}e_{i,k+r_i}^2\right]$$
$$- \alpha_i\beta_i\left[\boldsymbol{G}_i^{-\mathrm{T}}\boldsymbol{p}S_{i,k}\bar{b}_i(\boldsymbol{x}_k)\right]^{\mathrm{T}}\boldsymbol{G}_i[\boldsymbol{\Theta}_i^* - \boldsymbol{\Theta}_i(k)]$$
$$+ \frac{\alpha_i\beta_i^2}{2}\left[\boldsymbol{G}_i^{-\mathrm{T}}\boldsymbol{p}S_{i,k}\bar{b}_i(\boldsymbol{x}_k)\right]^{\mathrm{T}}\boldsymbol{G}_i\left[\boldsymbol{G}_i^{-\mathrm{T}}\boldsymbol{p}S_{i,k}\bar{b}_i(\boldsymbol{x}_k)\right]$$
$$+ \frac{1}{2}\left[\beta_i\left(\hat{g}_{i,k}(\boldsymbol{x}) - (\boldsymbol{\Theta}_i(k))^{\mathrm{T}}\boldsymbol{p}\right) + \alpha_i S_{i,k}\bar{b}_i(\boldsymbol{x}_k)\right]^2$$
$$- \frac{1}{2}\left[\hat{g}_{i,k}(\boldsymbol{x}) - (\boldsymbol{\Theta}_i(k))^{\mathrm{T}}\boldsymbol{p}\right]^2$$
$$= \alpha_i\beta_i\left[S_{i,a}(k) + S_{i,k}e_{i,k+r_i} + \frac{\lambda_{i,r_i}}{2}e_{i,k+r_i}^2\right]$$
$$- \alpha_i\beta_i S_{i,k}\bar{b}_i(\boldsymbol{x}_k)\left[\hat{g}_{i,k}^*(\boldsymbol{x}) - (\boldsymbol{\Theta}_i(k))^{\mathrm{T}}\boldsymbol{p}\right]$$
$$+ \frac{\alpha_i\beta_i^2}{2}\boldsymbol{p}^{\mathrm{T}}\boldsymbol{G}_i^{-\mathrm{T}}\boldsymbol{p}S_{i,k}^2\left(\bar{b}_i(\boldsymbol{x}_k)\right)^2 + \frac{1}{2}\left(\beta_i^2 - 1\right)$$
$$\cdot\left(\hat{g}_{i,k}(\boldsymbol{x}) - (\boldsymbol{\Theta}_i(k))^{\mathrm{T}}\boldsymbol{p}\right)^2 + \frac{1}{2}\alpha_i^2 S_{i,k}^2\left(\bar{b}_i(\boldsymbol{x}_k)\right)^2$$
$$+ \alpha_i\beta_i S_{i,k}\bar{b}_i(\boldsymbol{x}_k)\left[\hat{g}_{i,k}(\boldsymbol{x}) - (\boldsymbol{\Theta}_i(k))^{\mathrm{T}}\boldsymbol{p}\right].$$

Subsequently, by using Eq. (14) and substituting Eq. (18) into the above, we have

$$\Delta V_{i,k} = \varepsilon\alpha_i\beta_i S_{i,k}\bar{b}_i(\boldsymbol{x}_k) - \varepsilon_{i,h}\alpha_i\beta_i|S_{i,k}|\bar{b}_i(\boldsymbol{x}_k)$$
$$- \alpha_i\beta_i\left[k_{i,1}\bar{b}_i(\boldsymbol{x}_k) + k_{i,2}\left(\bar{b}_i(\boldsymbol{x}_k)\right)^2\right]|S_{i,k}|^2$$
$$+ \frac{\alpha_i\beta_i^2}{2}\boldsymbol{p}^{\mathrm{T}}\boldsymbol{G}_i^{-1}\boldsymbol{p}S_{i,k}^2\left(\bar{b}_i(\boldsymbol{x}_k)\right)^2 + \frac{1}{2}\alpha_i^2 S_{i,k}^2\left(\bar{b}_i(\boldsymbol{x}_k)\right)^2$$
$$+ \frac{1}{2}\left(\beta_i^2 - 1\right)\left[\hat{g}_{i,k}(\boldsymbol{x}) - (\boldsymbol{\Theta}_i(k))^{\mathrm{T}}\boldsymbol{p}\right]^2.$$

Because $0 < \beta_i < 1$ and $\varepsilon_{i,h} > |\varepsilon|$ (inequality (16)), the above equation satisfies

$$\Delta V_{i,k} \le -\alpha_i\beta_i\left[k_{i,1}\bar{b}_i(\boldsymbol{x}_k) + k_{i,2}\left(\bar{b}_i(\boldsymbol{x}_k)\right)^2\right]|S_{i,k}|^2$$
$$+ \frac{\alpha_i}{2}\left[\beta_i^2\boldsymbol{p}^{\mathrm{T}}\boldsymbol{G}_i^{-1}\boldsymbol{p} + \alpha_i\right]S_{i,k}^2\left(\bar{b}_i(\boldsymbol{x}_k)\right)^2. \tag{20}$$

It is known that $\boldsymbol{p}$ is the fuzzy basis of DFLS satisfying $\boldsymbol{p}^{\mathrm{T}}\boldsymbol{p} \le 1$. Then $\boldsymbol{p}^{\mathrm{T}}\boldsymbol{G}_i^{-1}\boldsymbol{p} \le \|\boldsymbol{G}_i\|^{-1}$. According to the parameter design conditions (16), inequality (20) is equivalent to

$$\Delta V_{i,k} \le -\alpha_i\beta_i k_{i,1}\bar{b}_i(\boldsymbol{x}_k)|S_{i,k}|^2,$$

which means that $\Delta V_{i,k}$ is negative semi-definite. $\Delta V_{i,k} \equiv 0$ holds if and only if $|S_{i,k}| \equiv 0$. $\forall\tilde{\boldsymbol{e}}_{i,k} \in \mathbb{R}^{r_i+1}$, $\|\boldsymbol{S}(k)\| \ne 0$, then $\Delta V_{i,k} < 0$.

According to the Lyapunov stability theory, the system error asymptotically converges to

$$\Omega_e \overset{\text{def}}{=} \left\{\tilde{\boldsymbol{e}}_{i,k} \mid |S_{i,k}| = 0\right\}.$$

Namely, the sliding mode can be reached.

After the state reaches the sliding mode, i.e., $S_{i,k} = 0$, the system error equation becomes

$$c_{i,r_i}e_{i,k+r_i-1} = -c_{i,1}e_{i,k} - c_{i,2}e_{i,k+1}$$
$$- \ldots - c_{i,r_i-1}e_{i,k+r_i-2}.$$

If $c_{i,j} > 0$ ($j = 1, 2, \ldots, r_i$) is Hurwitz, then the above $(r_i - 1)$th-order system is asymptotically stable. The same situation holds on every branch of the sliding surface $S_{i,k}$ for $i = 1, 2, \ldots, m$. As a result, the overall closed-loop system is asymptotically stable and the theorem is proved.

4.3 Chattering

Chattering reduction or elimination is dependent on the adaptive mechanism. The chattering signal of controller (15) in this study is produced by the nonlinear part

$$-\left\{\varepsilon_{i,h} + \left[k_{i,1} + k_{i,2}\bar{b}_i(\boldsymbol{x}_k)\right]|S_{i,k}|\right\}\mathrm{sgn}(S_{i,k}).$$

Fortunately, the part $[k_{i,1} + k_{i,2}\bar{b}_i(\boldsymbol{x}_k)]\,|S_{i,k}|$ exists only in the transient process. When $S_{i,k} = 0$, the chattering of controller (15) depends only on $\varepsilon_{i,h}$. Therefore, the chattering amplitude is determined only by $\varepsilon_{i,h}$.

Consequently, $\varepsilon_{i,h}$ is the switching signal to compensate the absolute error of the minimum approximation error between $g_{i,k}(\boldsymbol{x})$ and $\hat{g}^*_{i,k}(\boldsymbol{x})$ (defined by Eqs. (11) and (13)). Therefore, the chattering intensity is determined by the approximation ability of the DFLS. Because of the great approximation ability of the DFLS (the absolute approximation error can be arbitrarily small), parameter $\varepsilon_{i,h}$ can be designed to be very minor so that chattering is greatly reduced.

As we know, many efforts have been made to eliminate or weaken the chattering. For example, a famous chattering-weakening method can also be used, namely the saturation function:

$$\mathrm{sat}(S_{i,k}) = \begin{cases} 1, & S_{i,k} > \phi, \\ S_{i,k}/\phi, & |S_{i,k}| \le \phi, \\ -1, & S_{i,k} < -\phi, \end{cases}$$

where ϕ is called the boundary layer.

5 Simulation examples

5.1 A numerical example

A discrete mathematical model example is described as follows:

$$\begin{cases} y_{1,k+2} = y^2_{1,k+1} + (1.1 + 0.3\cos(2y_{2,k}))u_{1,k}, \\ y_{2,k+2} = y_{2,k} + \sqrt{y_{1,k+1}} + y^3_{2,k+1} + 1.3u_{2,k} \\ \qquad\qquad +0.3\cos(4\pi y_{1,k}). \end{cases} \tag{21}$$

The state of the system is $\boldsymbol{x}_k = [y_{1,k},\ y_{1,k+1},\ y_{2,k},\ y_{2,k+1}]^{\mathrm{T}}$ and the output is $\boldsymbol{y}_k = [y_{1,k},\ y_{2,k}]^{\mathrm{T}}$.

From the mathematical model (21), we can find the coupling between the two subsystems. Also, the nonlinear dynamics are unknown. The control design in this study will conquer them by the designed DFLS.

By using the proposed method, the estimations of the upper bounds of functions f_{1,u_1} and f_{2,u_2} are $\bar{b}_1(\boldsymbol{x}_k) = 1.4$ and $\bar{b}_2(\boldsymbol{x}_k) = 1.6$, according to Assumption 1 and Eq. (21). The disturbance or unmodeled dynamic is considered as $d(\boldsymbol{x}_k) = [0,\ 0.3\cos(4\pi y_{1,k})]^{\mathrm{T}}$.

A reference model is given as follows:

$$\begin{cases} y_{1,k+2} = -0.3y_{1,k+1} - 0.02y_{1,k} + r_1(k), \\ y_{2,k+2} = -0.3y_{2,k+1} - 0.02y_{2,k} + r_2(k). \end{cases}$$

The reference signals are $r_1(k) = r_2(k) = 0$. The sliding manifolds are

$$\begin{cases} S_{1,k} = x_2(k) + 0.1x_1(k), \\ S_{2,k} = x_4(k) + 0.05x_3(k). \end{cases}$$

The FSMC controller is designed as Eqs. (11), (15), (16) and the parameters of its adaptive law (17) are selected as $\alpha_1 = 0.3$, $\beta_1 = 0.1$, $\alpha_2 = 0.58$, $\beta_2 = 0.3$, and $\boldsymbol{G}_1 = \boldsymbol{G}_2 = \boldsymbol{I}$ (an identity matrix). The parameters of controller (15) are designed as $\varepsilon_{1,h} = \varepsilon_{2,h} = 0.01$, $k_{1,1} = 0.8$, $k_{1,2} = 1.6$, $k_{2,1} = 1.12$, and $k_{2,2} = 0.6$ by inequality (16). The Gaussian function is selected as the membership function for the DFLS.

Based on all the above-mentioned DFLS and control design, a relevant simulation is executed.

Figs. 3 and 4 show the curves of the output signals when the initial state is $\boldsymbol{x}_0 = [0.2,\ 0,\ 0.5,\ 0]^{\mathrm{T}}$. The two output signals are all asymptotically stable. Figs. 5 and 6 show the curves of the two sliding manifolds, which are also stable.

We set the sampling time of the designed DFLS, τ, to be 0.01 s. This is because the approximation can be guaranteed only if the DFLS output approximates to the nonlinear function within every sampling time interval of the system. Figs. 7 and 8 show the control input signals of the two subsystems. Parameters $\varepsilon_{i,h}$, $k_{i,1}$, and $k_{i,2}$ have imposed an important impact on the dynamic and stable performance. Parameter $\varepsilon_{i,h}$ processes mainly the approximation

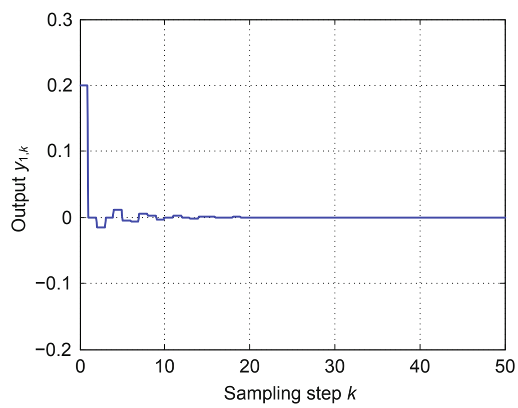

Fig. 3 Simulated output signal curve of $y_{1,k}$ (sampling time 0.1 s)

error of the DFLS. Furthermore, it determines the swing of the controller from Eq. (15). Parameters $k_{i,1}$ and $k_{i,2}$ mainly make the reaching of the sliding mode faster. Appropriate values of them are necessary and they can be obtained by an experimental approach.

From Figs. 3–8, it can be seen that there is no chattering either in state variables or in control signals. This is due to the filtering function of FLS for higher frequency signals.

5.2 An application to a robotic arm with two degrees of freedom

A robotic arm, which is widely applied to an industrial process, is the nonlinear and coupled nature of the dynamics (Lewis *et al.*, 2006). A robotic arm with two degrees of freedom (Fig. 9) is considered to visualize the contributions of this study. Its kinetic equation can be written as follows:

$$\boldsymbol{M}(\boldsymbol{q})\ddot{\boldsymbol{q}}+\boldsymbol{C}(\boldsymbol{q},\dot{\boldsymbol{q}})+\boldsymbol{G}(\boldsymbol{q})=\boldsymbol{T}, \tag{22}$$

where $\boldsymbol{q}=[\theta_1,\theta_2]^{\mathrm{T}}$ is the angular vector with θ_1 and θ_2 being the angular positions of the links, $\boldsymbol{M}(\boldsymbol{q})$ is

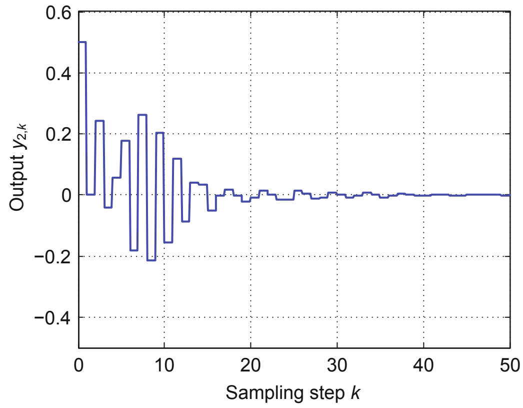

Fig. 4 Simulated output signal curve of $y_{2,k}$ (sampling time 0.1 s)

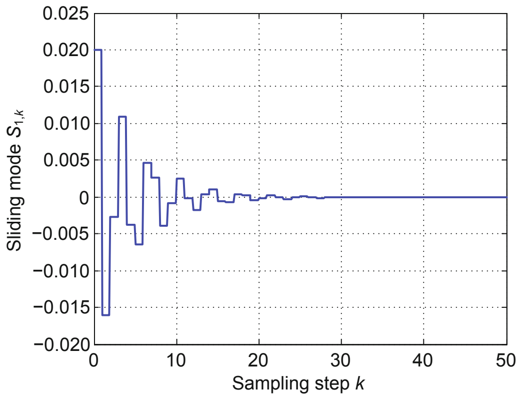

Fig. 5 Simulated sliding mode curve of $S_{1,k}$ (sampling time 0.1 s)

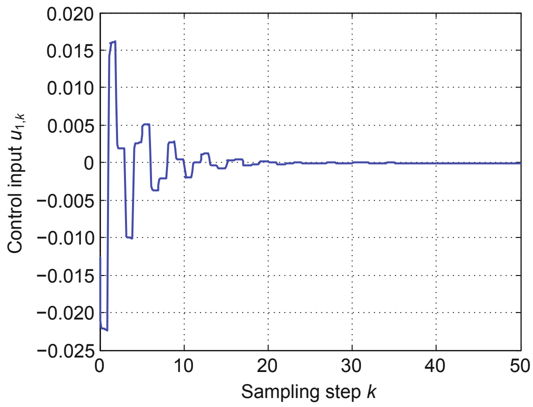

Fig. 7 Simulated control input signal curve of $u_{1,k}$ (DFLS sampling time 0.01 s)

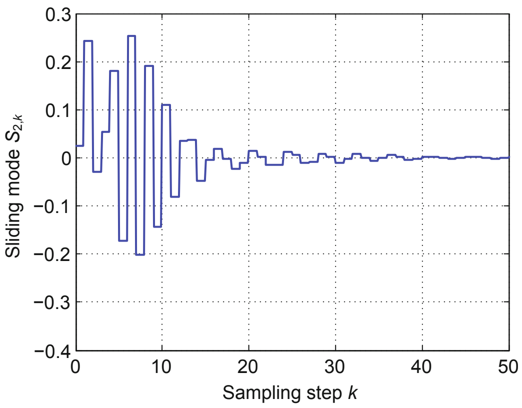

Fig. 6 Simulated sliding mode curve of $S_{2,k}$ (sampling time 0.1 s)

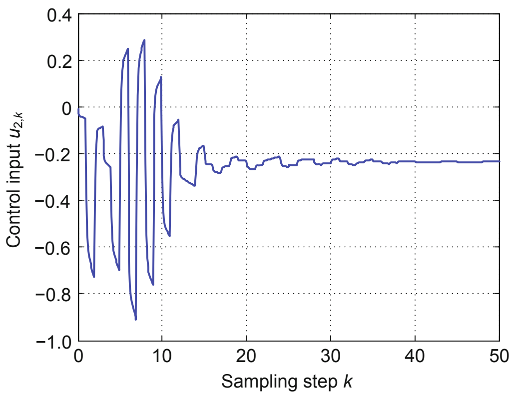

Fig. 8 Simulated control input signal curve of $u_{2,k}$ (DFLS sampling time 0.01 s)

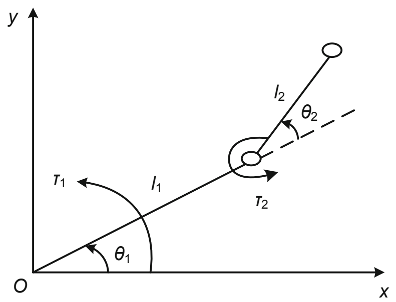

Fig. 9 Diagram of a robotic arm (with two degrees of freedom) with two drivings

the inertia matrix, $\boldsymbol{C}(\boldsymbol{q}, \dot{\boldsymbol{q}})$ represents the centrifugal and Coriolis torques, $\boldsymbol{G}(\boldsymbol{q})$ is the vector of gravitational torques, and $\boldsymbol{T} = [\tau_1, \tau_2]^{\mathrm{T}}$ is the vector of torques acting at the joints.

We assume that the gravitation of the two links is light enough to be neglected, i.e., $\boldsymbol{G}(\boldsymbol{q}) = \boldsymbol{0}$, and the matrices

$$\boldsymbol{M}(\boldsymbol{q}) = \begin{bmatrix} p_1 + 2p_3\cos\theta_2 & p_2 + p_3\cos\theta_2 \\ p_2 + p_3\cos\theta_2 & p_2 \end{bmatrix},$$

$$\boldsymbol{C}(\boldsymbol{q}, \dot{\boldsymbol{q}}) = \begin{bmatrix} -2p_3\dot{\theta}_1\dot{\theta}_2\sin\theta_2 - p_3\dot{\theta}_2^2\sin\theta_2 \\ p_3\dot{\theta}_1^2\sin\theta_2 \end{bmatrix},$$

where $p_1 = m_1r_1^2 + m_2(r_2^2 + l_1^2)$, $p_2 = m_2r_2^2$, and $p_3 = m_2l_1r_2$ with m_1 and m_2 being the masses of links 1 and 2 respectively, r_1 and r_2 the distances from the joint to the centers of masses of links 1 and 2 respectively, l_1 and l_2 the lengths of links 1 and 2 respectively. For a robotic arm model with two degrees of freedom, one may refer to Corradini *et al.* (2012). In this study, the parameters are set to $p_1 = 2.91$, $p_2 = 0.12$, and $p_3 = 0.18$.

By the general discretization technique, the discretization of Eq. (22) with a sampling time T_{s} can be given as follows:

$$\boldsymbol{q}_{k+2} = \boldsymbol{q}_{k+1} + T_{\mathrm{s}}(\boldsymbol{M}(\boldsymbol{q}_k))^{-1}\left[\boldsymbol{T} - \boldsymbol{C}(\boldsymbol{q}_k, \boldsymbol{q}_{k+1})\right], \tag{23}$$

where $\boldsymbol{q}_k = [\theta_{1,k}, \theta_{2,k}]^{\mathrm{T}}$ and

$$\boldsymbol{C}(\boldsymbol{q}_k, \boldsymbol{q}_{k+1}) = \frac{p_3\sin\theta_{2,k}}{T_{\mathrm{s}}^2}\begin{bmatrix} -2\Delta\theta_{1,k}\Delta\theta_{2,k} - \Delta\theta_{2,k}^2 \\ \Delta\theta_{1,k}^2 \end{bmatrix}$$

with $\Delta\theta_{1,k} = \theta_{1,k+1} - \theta_{1,k}$ and $\Delta\theta_{2,k} = \theta_{2,k+1} - \theta_{2,k}$. Obviously, model (23) is a typical example of Eq. (1), in which $\boldsymbol{q}_k$ is the output vector.

In this study, the sampling time of the robotic arm is 0.01 s. According to the controller design method we proposed, the sliding manifolds are designed as follows:

$$\begin{cases} S_{1,k} = \theta_{1,k+1} + 0.2\theta_{1,k}, \\ S_{2,k} = \theta_{2,k+1} + 0.1\theta_{2,k}. \end{cases}$$

The FSMC controller is designed as Eqs. (11), (15), and (16), and the parameters of its adaptive law (17) are selected as $\alpha_1 = 2$, $\beta_1 = 0.1$, $\alpha_2 = 0.1$, $\beta_2 = 0.2$, $\boldsymbol{G}_1 = \boldsymbol{I}$, and $\boldsymbol{G}_2 = 2\boldsymbol{I}$. The parameters of controller (15) are designed as $\varepsilon_{1,h} = \varepsilon_{2,h} = 0.01$, $k_{1,1} = 4$, $k_{1,2} = 3$, $k_{2,1} = 1$, and $k_{2,2} = 0.8$ by inequality (16). The Gaussian function is selected as the membership function for the DFLS. The estimations of the upper bounds for the control gains are $\bar{b}_1(\boldsymbol{q}_k) = 0.4$ and $\bar{b}_2(\boldsymbol{q}_k) = 1$. The reference model to be tracked is given as follows:

$$\begin{cases} \theta_{\mathrm{d}1,k+2} = 0.3\theta_{\mathrm{d}1,k+1} + 0.1\theta_{\mathrm{d}1,k} + r_1(k), \\ \theta_{\mathrm{d}2,k+2} = 0.3\theta_{\mathrm{d}2,k+1} + 0.1\theta_{\mathrm{d}2,k} + r_2(k), \end{cases}$$

where $\theta_{\mathrm{d}1,k}$ and $\theta_{\mathrm{d}2,k}$ are the angular positions to be tracked.

First, the reference trajectories are step signals, i.e., $r_1(k) = r_2(k) = 1$. The simulation results are obtained under the initial positions $\theta_1(0) = 0$, $\theta_2(0) = 0$. Figs. 10 and 11 show the angular positions of the robotic arm. Figs. 12 and 13 show the sliding manifolds and the control torques, respectively. From Figs. 10–13, it can be seen that the robotic arm has fast response and the control torques have no chattering. These simulation results validate the effectiveness of the method.

Furthermore, the reference trajectories are replaced by $r_1(k) = 0.5\sin t$ and $r_2(k) = 0.4\cos t$. To increase the convergence speed of the sliding

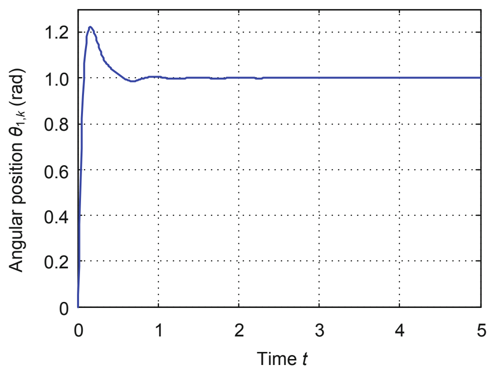

Fig. 10 Angular position curve $\theta_{1,k}$ (sampling time 0.01 s)

manifolds, the estimations of the upper bounds for the control gains are set to $\bar{b}_1(\boldsymbol{q}_k) = \bar{b}_2(\boldsymbol{q}_k) = 5$, and the parameters of controller (15) are changed to $k_{1,1} = 10$, $k_{1,2} = 2$, $k_{2,1} = 5$, and $k_{2,2} = 1$. The tracking performance under the initial positions $\theta_1(0) = 0.5$, $\theta_2(0) = 0$ are shown in Figs. 14–18.

The sampling time of the designed DFLS, τ, is 0.001 s. In Fig. 18, the control torque signals of the two links are continuous, which validates the chattering-free performance. The tracking errors in Fig. 16 converge very quickly. As mentioned before, parameters $k_{i,1}$ and $k_{i,2}$ have imposed an important impact on the dynamic and stable

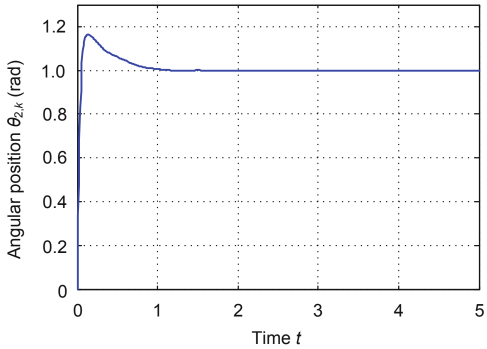

Fig. 11 Angular position curve $\theta_{2,k}$ (sampling time 0.01 s)

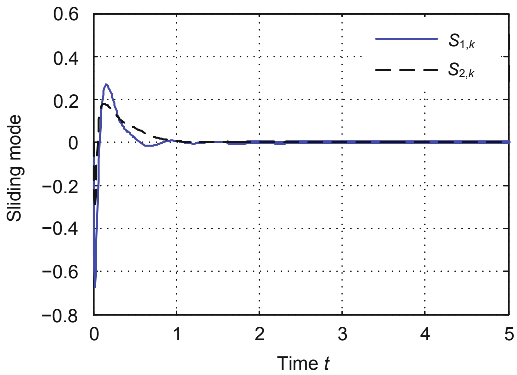

Fig. 12 Sliding mode curves: $S_{1,k}$ and $S_{2,k}$ (sampling time 0.01 s)

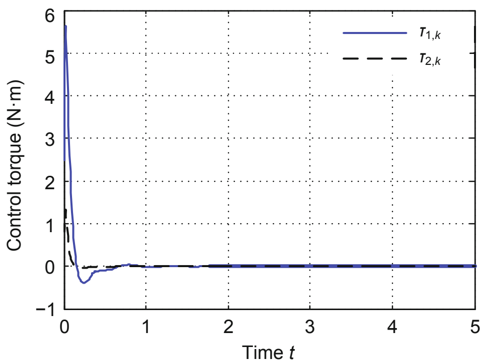

Fig. 13 Control torque curves: $\tau_{1,k}$ and $\tau_{2,k}$ (DFLS sampling time 0.001 s)

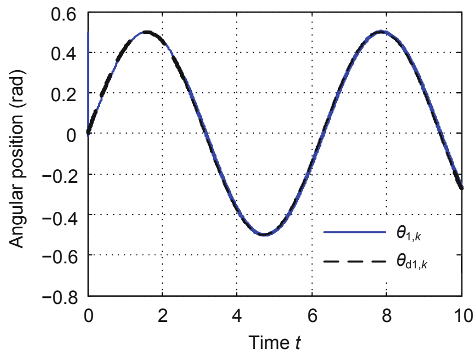

Fig. 14 Tracking curves of link 1: $\theta_{1,k}$ and $\theta_{d1,k}$ (DFLS sampling time 0.001 s)

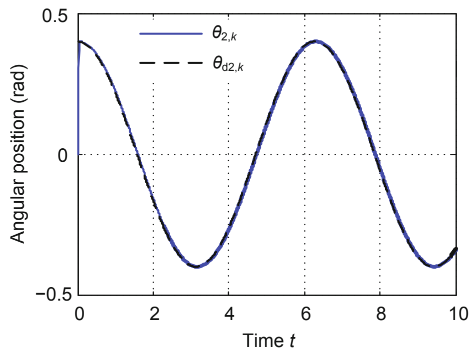

Fig. 15 Tracking curves of link 2: $\theta_{2,k}$ and $\theta_{d2,k}$ (DFLS sampling time 0.001 s)

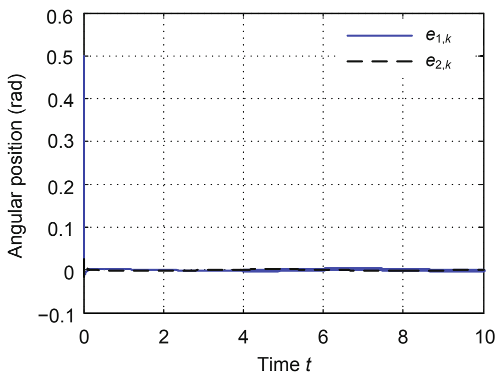

Fig. 16 Tracking error curves: $e_{1,k}$ and $e_{2,k}$ (DFLS sampling time 0.001 s)

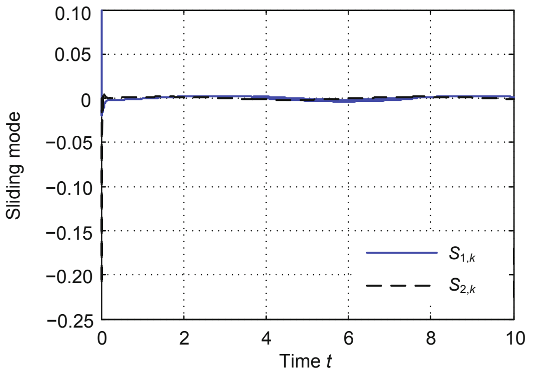

Fig. 17 Sliding mode curves of links 1 and 2: $S_{1,k}$ and $S_{2,k}$ (sampling time 0.01 s)

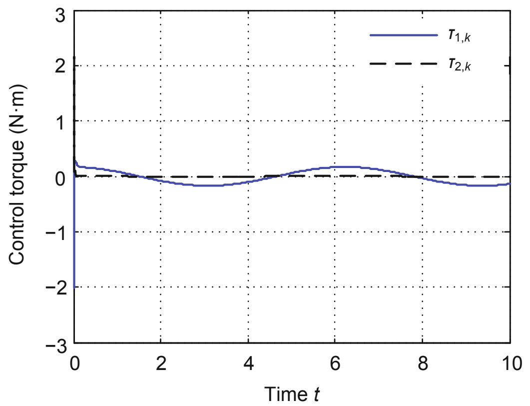

Fig. 18 Control torque curves of links 1 and 2: $\tau_{1,k}$ and $\tau_{2,k}$ (DFLS sampling time 0.001 s)

performance. Hence, their values are selected a little larger in this application. These simulation results certificate the good performance of the proposed method.

6 Conclusions

An adaptive FSMC design method for a class of non-affine discrete nonlinear systems has been proposed in this paper. The sliding mode control was designed based on the DFLS, which has strongly arbitrary approximation properties of the unmodeled dynamics. The appropriate adaptive mechanism guarantees the stability of the closed-loop system. Due to the use of the DFLS, the chattering of the SMC has been greatly weakened, whereas the robustness has been retained. Finally, the presented simulation results have validated the good performance of the proposed method.

References

Allaoua, B., Laoufi, A., 2013. A novel sliding mode fuzzy control based on SVM for electric vehicles propulsion system. *Energy Procedia*, **36**:120-129. http://dx.doi.org/10.1016/j.egypro.2013.07.015

Castillo-Toledo, B., di Gennaro, S., Loukianov, A.G., *et al.*, 2008. Discrete time sliding mode control with application to induction motors. *Automatica*, **44**(12):3036-3045. http://dx.doi.org/10.1016/j.automatica.2008.05.009

Chen, D., Liu, Y., Ma, X., *et al.*, 2012a. Control of a class of fractional-order chaotic systems via sliding mode. *Nonl. Dyn.*, **67**(1):893-901. http://dx.doi.org/10.1007/s11071-011-0002-x

Chen, D., Zhang, R., Sprott, J.C., *et al.*, 2012b. Synchronization between integer-order chaotic systems and a class of fractional-order chaotic system based on fuzzy sliding mode control. *Nonl. Dyn.*, **70**(2):1549-1561. http://dx.doi.org/10.1007/s11071-012-0555-3

Corradini, M.L., Fossi, V., Giantomassi, A., *et al.*, 2012. Discrete time sliding mode control of robotic manipulators: development and experimental validation. *Contr. Eng. Pract.*, **20**(8):816-822. http://dx.doi.org/10.1016/j.conengprac.2012.04.005

Edwards, C., Spurgeon, S., 1998. Sliding Mode Control: Theory and Applications. CRC Press.

Farhoud, A., Erfanian, A., 2014. Fully automatic control of paraplegic FES pedaling using higher-order sliding mode and fuzzy logic control. *IEEE Trans. Neur. Syst. Rehabil. Eng.*, **22**(3):533-542. http://dx.doi.org/10.1109/TNSRE.2013.2296334

Furuta, K., 1990. Sliding mode control of a discrete system. *Syst. Contr. Lett.*, **14**(2):145-152. http://dx.doi.org/10.1016/0167-6911(90)90030-X

Guo, L., Hung, J.Y., Nelms, R.M., 2011. Comparative evaluation of sliding mode fuzzy controller and PID controller for a boost converter. *Electr. Power Syst. Res.*, **81**(1):99-106. http://dx.doi.org/10.1016/j.epsr.2010.07.018

Ho, T.H., Ahn, K.K., 2012. Speed control of a hydraulic pressure coupling drive using an adaptive fuzzy sliding-mode control. *IEEE/ASME Trans. Mechatron.*, **17**(5):976-986. http://dx.doi.org/10.1109/TMECH.2011.2153866

Hsu, C.F., Chung, I.F., Lin, C.M., 2009. Self-regulating fuzzy control for forward DC-DC converters using an 8-bit microcontroller. *IET Power Electron.*, **2**(1):1-12. http://dx.doi.org/10.1049/iet-pel:20070179

Hwang, C.L., Wu, H.M., Shih, C.L., 2009. Fuzzy sliding-mode underactuated control for autonomous dynamic balance of an electrical bicycle. *IEEE Trans. Contr. Syst. Technol.*, **17**(3):658-670. http://dx.doi.org/10.1109/TCST.2008.2004349

Khandekar, A.A., Malwatkar, G.M., Patre, B.M., 2013. Discrete sliding mode control for robust tracking of higher order delay time systems with experimental application. *ISA Trans.*, **52**(1):36-44. http://dx.doi.org/10.1016/j.isatra.2012.09.002

Lee, J.X., Vukovich, G., 1997. Identification of nonlinear dynamic systems—a fuzzy logic approach and experimental demonstrations. Proc. IEEE Int. Conf. on Systems, Man, and Cybernetics, p.1121-1126. http://dx.doi.org/10.1109/ICSMC.1997.638100

Lewis, F.L., Dawson, D.M., Abdallah, C.T., 2006. Robot Manipulator Control: Theory and Practice. Marcel Dekker, Inc., USA.

Lian, Y., Gómez, G., Masdemont, J.J., *et al.*, 2014. Station-keeping of real Earth-Moon libration point orbits using discrete-time sliding mode control. *Commun. Nonl. Sci. Numer. Simul.*, **19**(10):3792-3807. http://dx.doi.org/10.1016/j.cnsns.2014.03.026

Monsees, G., Scherpen, J.M.A., 2002. Adaptive switching gain for a discrete-time sliding mode controller. *Int. J. Contr.*, **75**(4):242-251. http://dx.doi.org/10.1080/00207170110101766

Morioka, H., Wada, K., Sabanovic, A., *et al.*, 1995. Neural network based chattering free sliding mode control. Proc. 34th SICE Annual Conf., p.1303-1308. http://dx.doi.org/10.1109/SICE.1995.526699

Pai, M.C., 2014. Discrete-time output feedback quasi-sliding mode control for robust tracking and model following of uncertain systems. *J. Franklin Inst.*, **351**(5):2623-2639. http://dx.doi.org/10.1016/j.jfranklin.2014.01.005

Pande, V.N., Mate, U.M., Kurode, S., 2013. Discrete sliding mode control strategy for direct real and reactive power regulation of wind driven DFIG. *Electr. Power Syst. Res.*, **100**:73-81. http://dx.doi.org/10.1016/j.epsr.2013.03.001

Poursamad, A., Davaie-Markazi, A.H., 2009. Robust adaptive fuzzy control of unknown chaotic systems. *Appl. Soft Comput.*, **9**(3):970-976. http://dx.doi.org/10.1016/j.asoc.2008.11.014

Reddy, G.D., Park, Y., Bandyopadhyay, B., *et al.*, 2009. Discrete-time output feedback sliding mode control for spatial control of a large PHWR. *Automatica*, **45**(9):2159-2163. http://dx.doi.org/10.1016/j.automatica.2009.05.003

Sarpturk, S.Z., Istefanopulos, Y., Kaynak, O., 1987. On the stability of discrete-time sliding mode control systems. *IEEE Trans. Autom. Contr.*, **32**(10):930-932.

Shahraz, A., Boozarjomehry, R.B., 2009. A fuzzy sliding mode control approach for nonlinear chemical processes. *Contr. Eng. Pract.*, **17**(5):541-550. http://dx.doi.org/10.1016/j.conengprac.2008.10.011

Sira-Ramirez, H., 1989. Nonlinear variable structure systems in sliding mode: the general case. *IEEE Trans. Autom. Contr.*, **34**(11):1186-1188. http://dx.doi.org/10.1109/9.40749

Utkin, V.I., 1977. Variable structure systems with sliding modes. *IEEE Trans. Autom. Contr.*, **22**(2):212-222. http://dx.doi.org/10.1109/TAC.1977.1101446

Wang, L., 1995. Design and analysis of fuzzy identifiers of nonlinear dynamic systems. *IEEE Trans. Autom. Contr.*, **40**(1):11-23. http://dx.doi.org/10.1109/9.362903

Wang, S., Yu, D., 2000. Error analysis in nonlinear system identification using fuzzy system. *J. Softw.*, **11**(4):447-452.

Wang, W., Liu, X., 2010. Fuzzy sliding mode control for a class of piezoelectric system with a sliding mode state estimator. *Mechatronics*, **20**(6):712-719. http://dx.doi.org/10.1016/j.mechatronics.2010.06.009

Yau, H.T., Wang, C.C., Hsieh, C.T., *et al.*, 2011. Nonlinear analysis and control of the uncertain micro-electro-mechanical system by using a fuzzy sliding mode control design. *Comput. Math. Appl.*, **61**(8):1912-1916. http://dx.doi.org/10.1016/j.camwa.2010.07.019

Zhang, D.Q., Panda, S.K., 1999. Chattering-free and fast response sliding mode controller. *IEE Proc. Contr. Theory Appl.*, **146**(2):171-177. http://dx.doi.org/10.1049/ip-cta:19990518

Zhang, X., 2009. Adaptive sliding mode-like fuzzy logic control for nonlinear systems. *J. Commun. Comput.*, **6**(1):53-60.

Zhang, X., Guo, F., 2014. Sliding mode-like fuzzy logic control with boundary layer self-tuning for discrete nonlinear systems. Proc. 7th Int. Conf. on Intelligent Systems and Knowledge Engineering, p.479-490. http://dx.doi.org/10.1007/978-3-642-37829-4_41

Zhang, X., Su, H.Y., 2004. Sliding mode variable structure state norm control of SISO linear systems. *Contr. Eng. China*, **11**(5):413-418 (in Chinese).

Zhang, X., Chen, W., Shen, B., 2015. Direct adaptive fuzzy sliding mode control for a class of non-affine discrete nonlinear systems. Proc. 12th Int. Conf. on Fuzzy Systems and Knowledge Discovery, p.355-360. http://dx.doi.org/10.1109/FSKD.2015.7381962

Zhu, M.C., Li, Y.C., 2010. Decentralized adaptive fuzzy sliding mode control for reconfigurable modular manipulators. *Int. J. Robust Nonl. Contr.*, **20**(4):472-488. http://dx.doi.org/10.1002/rnc.1444